UCSF
UC San Francisco Electronic Theses and Dissertations

Title
Altering Osteoclasts In Utero Leads to Changes in Mandibular Lengths in Adult Mice

Permalink
https://escholarship.org/uc/item/5ps120h4

Author
Vargas, Ricardo Luis

Publication Date
2019

Peer reviewed|Thesis/dissertation

eScholarship.org Powered by the California Digital Library
University of California

Altering Osteoclasts In Utero Leads to Changes in Mandibular Lengths in Adult Mice

by
Ricardo Luis Vargas

THESIS
Submitted in partial satisfaction of the requirements for degree of
MASTER OF SCIENCE

in

Oral and Craniofacial Sciences

in the

GRADUATE DIVISION
of the
UNIVERSITY OF CALIFORNIA, SAN FRANCISCO

Approved:

DocuSigned by:
Andrew H. Jheon
F365EA7416024CA...
Andrew H. Jheon
Chair

DocuSigned by:
Nathan Young
Nathan Young

DocuSigned by:
Richard A. Schneider
C704CE82E8E34CE...
Richard A. Schneider

Committee Members

Acknowledgements

MGH was supported by the Fulbright Program and AMIDEAST. AHJ was supported in part by the UCSF Clinical and Translational Science Institute (CTSI) Pilot Fund program (RAS #A127552). All authors declare that there are no conflicts of interest. This study was funded in part by the UCSF Clinical and Translational Science Institute (CTSI) Pilot Fund program (RAS #A127552) to AHJ, and MGH was supported by the Fulbright Program and AMIDEAST

Altering Osteoclasts In Utero Leads to Changes in Mandibular Lengths in Adult Mice

Ricardo Vargas

Abstract

Craniofacial skeletal malocclusions often involve the hyper- or hypo-morphogenesis of the maxilla and/or mandible. Although genetic and environmental factors are thought to play important roles in the etiology of skeletal malocclusions, specific contributions of either factor are yet unclear. To determine whether alterations in osteoclastic activity during embryonic/fetal development changes lead to changes in mammals jaw lengths, we utilized three mouse models to alter osteoclast activity during development. First, we injected *in vivo* siRNA specific to cathepsin K (*Ctsk*), a gene expressed highly in osteoclasts to decrease *Ctsk* and in turn, osteoclast activity in pregnant dams at embryonic day 12.5. Second, we generated genetically modified $Ctsk^{Cre}$;$DTA^{fl/+}$ (diphtheria toxin A) mice, which led to an increase in osteoclasts. Third, we fed Time-mated FVB wildtype mice high calcium and low phosphorous diets during gestation. Changes in offspring osteoclast activity were confirmed by tartrate-resistant acid phosphatase (TRAP) assay. Micro-computed tomography and three-dimensional (3D) geometric morphometrics revealed changes to 6-week old mouse craniofacial morphology. Downregulation of *Ctsk* by siRNA led to decreased osteoclast activity and was associated with an increase in mandibular body length. Conversely, an increase in osteoclast activity in $Ctsk^{Cre}$;$DTA^{fl/+}$mice was associated with a decrease in mandibular body length. Increased calcium and decreased phosphorus levels in utero led to a retrognathic mandible associated with lowered BMD in experimental females, whereas experimental males showed partly opposite effects Our study demonstrates that

alterations in osteoclast activity during gestation leads to 3D shape changes in the adult mandible.

TABLE OF CONTENTS

Chapter 1. Introduction *1*

Chapter 2. Perturbation of osteoclasts in utero via Ctsk siRNA or Ctsk^{Cre};DTA$^{fl/+}$ mice affects mouse craniofacial morphology 7

2.1 *Introduction* *7*

2.2 *Materials and Methods* *10*

2.3 *Results* *14*

2.4 *Discussion* *17*

Chapter 3. Altering calcium and phosphorus levels in utero affects adult mouse mandibular morphology 25

3.1 *Introduction* *26*

3.2 Materials and Methods *28*

3.3 *Results* *31*

3.4 *Discussion* *34*

3.5 Conclusion *37*

References *43*

LIST OF FIGURES

Fig. 2.1 *In vivo* siRNA knockdown of *Ctsk in utero* leads to changes in osteoclast activity and 3D morphological differences 20

Fig. 2.2 *In vivo* siRNA knockdown of *Ctsk in utero* is associated with a lengthening of the mandibular body using geometric morphometrics analysis 21

Fig. 2.3 *Ctsk*^{Cre};DTA$^{fl/+}$ mutant mice show an increase in osteoclast activity and 3D morphological differences. (A) Experimental design 22

Fig. 2.4 An increase in osteoclast activity in *Ctsk*^{Cre};DTA$^{fl/+}$ mutant mice is associated with a shortening of the mandibular body using geometric morphometrics analysis 23

Fig. 2.5 Landmarks of Mouse Skull 24

Fig. 3.1 Principal components analysis (PCA) of regression residuals of shape variation in the mandible 38

Fig. 3.2 Principal components analysis (PCA) of regression residuals of shape variation in the condyle 39

Fig. 3.3 Canonical variate analysis (CVA) of the mandibular condyles 41

Fig. 3.4 Mouse mandible and landmarks 40

LIST OF TABLES

Table 3.1 Bone mineral density measurements 42

Chapter 1. Introduction

Class I, II, and III malocclusions were classified based on maxillary and mandibular permanent molar relationships by Edward H. Angle in 1899 (1). Jaw relationship discrepancies, morphology, and other anomalies of the mandible and maxilla contribute to skeletal malocclusions associated with their corresponding angle classification. An important role of orthodontists is to determine the skeletal and dental contributions in malocclusion. Class II and III skeletal malocclusions are often difficult to correct. Commonly in skeletal malocclusions, orthognathic surgery and/or extractions are required, which lead to increased treatment and doctor chair time. It has been reported that class III malocclusions range from 10-16% in Asian populations (2), whereas in Caucasian populations class II malocclusions arise in 23% of the population and Class III in 3.4% (3). With better understanding of the etiology of skeletal malocclusions, we may devise treatments that prevent or lessen these malocclusions.

The etiology of skeletal malocclusions is not well understood. In the past, malocclusions were believed to be the result of endocrine malfunction, “pressure habits,” dietary deficiencies, or even mental degeneracy (4). It was not until the 1960’s that genetics began being considered a factor contributing to malocclusions (4,5). Numerous familial aggregation studies demonstrate the role of genetics in class II and III malocclusions (6,7). For example, matrix protein matrilin-1 (*MATN1*), collagen type 1A (*COLIAI*), and cartilage and fibroblast growth factor 2 (*FGFR2*) were associated with increased risk of Class III malocclusion, whereas T-Box 5 (*TBX5*) was associated with decreased risk of Class III malocclusion (8). Perillo et al. (2015) analyzed the genetic composition of an Italian family using whole-exome sequencing of which 30% of the

family members presented with class III malocclusions. In this prior study, five genes with missense variants were identified to be shared by all of the prognathic family members, one of which was the Gly1121Ser variant in ARHGAP21 (Rho GTPase Activating Protein 21) (9). Ikuno *et al.* (2014) identified two chromosome regions (1q32.2 and 1p22.3) to be likely susceptible regions of mandibular prognathism. Plexin A2 (*PLXNA2*) and Synovial Sarcoma, X Breakpoint 2 Interacting Protein (*SSX2IP*) were closely associated with these two chromosome regions and had previously not been linked to craniofacial growth (8,9,10) In addition, despite these reports of several candidate genes involved in skeletal malocclusions, environmental factors (excluding trauma and pathologies) also likely play an important role in skeletal malocclusions and craniofacial morphology determination (11). Variations in masticatory behavior have been hypothesized to lead to changes in skull size and morphology. For example, shifts in subsistence strategy from foraging to farming led to wider cultural changes including increased food processing and consumption of softer diet (12). Likewise, the transition to softer diets following the Industrial Revolution is associated with a measurable decrease in mandible size (12). Soft diets are believed to be one of the primary factors in inducing morphological changes to the mandible (13), and dramatic reductions in the sizes of the face and jaws were observed wherever humans transitioned from foraging to farming (11).

Regardless of the etiology of skeletal malocclusions, jaw development requires bone-forming osteoblasts and bone-resorbing osteoclasts which are responsible for bone formation and turnover (14). Osteoblasts secrete extracellular matrix that eventually mineralizes to form bone. Bone turnover, where old bone is replaced with

new bone occurs continuously throughout life, requires precise control and balance, and occurs immediately upon initial mineralization, as evidenced by the presence of markers of osteoclasts (5). Interestingly, osteoclasts are present even before mineralization (5). An imbalance between osteoblast/osteoclast activity may lead to downstream effects such as osteopetrosis, a rare condition in which bone is abnormally dense and prone to fractures, and osteoporosis, a metabolic bone disease where osteoclast activity exceeds osteoblast activity leading to decreased bone density. However, very little is known about the role of osteoblasts and osteoclasts in the morphogenesis of the mandible.

The role of osteoclasts as a determinant of avian beak length was previously reported after significantly higher tartrate-resistant acid phosphatase (TRAP) activity, an indicator of osteoclasts and their activity was observed in developing small-beaked quails compared to long-beaked ducks (15). In this prior study, the investigators used quails, which have short and sharp beaks to test whether osteoclast number plays a role in beak length determination (15). Alendronate (bisphosphonate), osteoprotegerin (OPG) protein, or metallomatrix proteinase-13 (MMP-13) inhibitor were injected *in ovo* in a single dose to the blood vessels of quail embryos, which resulted in decreased osteoclast number before craniofacial bone mineralization (15). An increase in lower beak length in all three of these treatment modalities was observed with a decrease in osteoclasts (15). Conversely, increasing the osteoclast number via injection of recombinant receptor activator of nuclear factor kappa-B ligand (rRANKL) resulted in shorter lower beak lengths. These observations demonstrated the importance and role

of osteoclasts in determining lower beak length. However, the importance and role of osteoclasts in mammalian mandibles is still unknown.

To elucidate the role of osteoclasts in the development of the mammalian mandible, cathepsin K (*Ctsk*) may be targeted. CTSK is encoded by the *Ctsk* gene on chromosome 1q21 and is a member of the papain-like cysteine protease family (16). CTSK is a lysosomal protease that plays a role in numerous physiological processes such as bone remodeling, keratinocyte differentiation, prohormone activation, and MHC-II-mediated antigen presentation (17). *Ctsk* is lowly expressed in the heart, lung, colon, ovary, skeletal muscle, and placenta whereas it is highly expressed in osteoclasts. Its function within osteoclasts is to degrade bone matrix proteins such as osteonectin, osteopontin, and type I collagen (18). The integral role of *Ctsk* in bone resorption via regulation of osteoclast activity has previously been confirmed in mammals such as mice and humans (17). Thus, targeting *Ctsk* would allow for osteoclast activity to be altered in the mammalian mandible and the resulting changes in the mammalian mandibles, specifically in mice, will be analyzed in this study.

One method to alter the number of osteoclasts during mouse development is to use mice carrying the *Ctsk* Cre^{+} allele. Transgenic mouse lines such as Cre have two different methods of production; transgenesis with DNA pronuclear injection, or knock-in with homologous recombination in embryonic stem cells (19). The Cre-*loxP* system is a method of gene targeting that allows inactivation of a specific target gene in mice. The use of an interferon-responsive promoter that controls the expression of Cre recombinase to delete a segment of the DNA polymerase beta gene that is flanked by *loxP*recombinase recognition sites (20). This system helps to prevent secondary effects,

lethal consequences, and over expression of proteins all causing altered phenotypes (19). Thus, mice carrying the *Ctsk*^{Cre} (6) and ROSA26^{DTA176} (7) alleles were mated to generate *Ctsk*^{Cre};DTA$^{fl/+}$ offspring, which would lead to ablation of *Ctsk*$^{+}$ cells or osteoclasts.

A second method to alter the number of osteoclasts during mouse development is to administer small interfering RNA (siRNA) specific for *Ctsk* via *in vivo* injection during mouse embryogenesis. siRNA regulates gene expression via RNA interference (21). This ability to inhibit specific genes has increased siRNA's popularity for use in biomedical research (21). siRNAs can be introduced into cells as exogenous double-stranded RNA (dsRNA) or by nuclear transcription of micro-RNA (miRNA) genes. The RNAs are cleaved into 21–23 nucleotide (nt) siRNAs by an enzyme Dicer. After processing, the siRNAs are incorporated into a multiprotein complex called the RNA-induced silencing complex (RISC). The target RNA is then degraded, or translation is arrested due to base pairing (22). There are different strategies used to deliver dsRNAs to cells which include directly or by introduction of expression vectors (22).

A third method to test the role of osteoclasts on the development of the mammalian mandible is diet. Osteoclasts are sensitive to calcium and phosphorus levels, and excessive calcium levels can impair bone mineralization and growth due to decreased efficacy of phosphorus absorption (23). In addition, phosphorus deficiency may lead to increased osteoclast number and size (24). Hence, altering the maternal mouse diet to have excess calcium and deficient phosphorus levels during gestation may affect the development of the mammalian mandible.

After the osteoclast activity has been altered by these different approaches, the mammalian mandible can be analyzed using geometric morphometrics. Geometric morphometrics is a robust statistical technique that has been used in different biological fields for the study of changes in shape and how it relates to underlying variables (25). Geometric morphometrics has been gaining in popularity becoming a powerful tool that has been increasingly used in the last two decades, specifically in dental sciences such as orthodontics (25). Landmark sets were used, and the Procrustes coordinates enabled correction for shape variables (25). To analyze the shape variation of each sample, a principal component analysis was done using MorphoJ software. Allometric shape changes were explored using multivariate regression of variables against centroid size in MorphoJ.

In this thesis, I present two complete manuscripts. The first manuscript or Chapter 2 of my thesis is entitled, “Perturbation of osteoclasts *in utero* via *Ctsk* siRNA or *Ctsk*^{Cre};DTA$^{fl/+}$ mice affects mouse craniofacial morphology.” In this study, we altered the number of osteoclasts by generating *Ctsk*^{Cre};DTA$^{fl/+}$ mice and by administrating *in vivo* siRNA specific to *Ctsk* via injection during mouse embryogenesis. The second manuscript or Chapter 3 of my thesis is entitled, “Altering calcium and phosphorus levels in utero affects adult mouse mandibular morphology.” The purpose of both manuscripts was to determine whether mice with decreased osteoclast number would lead to three-dimensional (3D) morphological changes in mammalian mandibular lengths. In summary, we discovered that increased osteoclast activity led to shorter mandibles whereas decreased osteoclast activity led to longer mandibles.

Chapter 2: Perturbation of osteoclasts *in utero* via *Ctsk* siRNA or *Ctsk*^{Cre};DTA$^{fl/+}$ mice affects mouse craniofacial morphology

Introduction

Class I, II, and III malocclusions are classified based on maxillary and mandibular permanent molar relationships by Edward H. Angle in 1899 (26). An important role of orthodontists is to determine the skeletal and dental contributions in malocclusion. Class II and III skeletal malocclusions are often difficult to correct requiring extractions and/or orthognathic surgery. With better understanding of the etiology of skeletal malocclusions, we may be able to devise treatments that prevent or lessen these malocclusions.

Malocclusion was believed to be the result of endocrine malfunction, pressure habits, dietary deficiencies, or even mental degeneracy (4). To date, numerous familial aggregation studies have demonstrated the potential roles of specific genes in class II and III malocclusion (6,7). For example, matrix protein matrilin-1 (*MATN1*), collagen type 1A (*COLIAI*), fibroblast growth factor 2 (*FGFR2*), the Gly1121Ser variant in ARHGAP21 (Rho GTPase Activating Protein 21), Plexin A2 (*PLXNA2*) and Synovial Sarcoma, X Breakpoint 2 Interacting Protein (*SSX2IP*) have been associated with increased risk of mandibular prognathism or Class III malocclusion (8,9,10). However, beyond genetic influences, environmental factors also play a role in craniofacial morphology determination. Variations in masticatory behavior have been hypothesized to lead to changes in skull size and morphology. For example, shifts in subsistence strategy from foraging to farming led to wider cultural changes including increased food

processing and consumption of softer diets (11). Likewise, the transition to softer diets following the Industrial Revolution is associated with a measurable decrease in mandible size (12). Soft diets are believed to be one of the primary factors in inducing morphological changes to the mandible (13), and dramatic reductions in the sizes of the face and jaws were observed wherever humans transitioned from foraging to farming (11).

Bone-forming osteoblasts and bone-resorbing osteoclasts are the two major cells required for bone formation and turnover (14). The role of osteoclasts as a determinant of avian beak length was previously reported after significantly higher tartrate-resistant acid phosphatase (TRAP) activity, an indicator of osteoclast activity was observed in developing small-beaked quails compared to large-billed ducks (15). When the bisphosphonate alendronate, osteoprotegerin (OPG) protein, or MMP-13 (metallomatrix proteinase-13) inhibitor was injected into the blood vessel of developing quail embryos before mineralization of the craniofacial bones, all three treatments led to decreased craniofacial osteoclast activity and increased lower beak length. Conversely, increased osteoclast activity via injection of recombinant RANKL (receptor activator of nuclear factor kappa-B ligand), an activator of osteoclastogenesis resulted in shorter lower beak lengths.

The purpose of our study was to determine whether altering osteoclast activity *in utero* would lead to three-dimensional (3D) morphological changes in adult mouse mandibles and skulls. To alter osteoclast activity, we targeted cathepsin K (*Ctsk*), a selective marker of bone resorption highly expressed in osteoclasts (16,27) using two methods: injection of *in vivo* siRNA specific to *Ctsk* and generation of genetically

modified mice where cells expressing *Ctsk*, primarily osteoclasts are eliminated. We determined that an increase in osteoclast activity during gestation was associated with a shortened adult mandibular body, whereas a decrease in osteoclast activity was associated with a longer mandibular body. Our data demonstrate that changes in osteoclast activity at specific stages of development may lead to or worsen Class II or Class III skeletal malocclusion.

Material and Methods

In vivo siRNA injection and genetically modified mice

All aspects of animal care and experiments were approved by the Institutional Animal Care and Use Committee (IACUC). Timed-pregnant FVB mice at embryonic day (E) 12.5 were injected with *in vivo* siRNA specific for *Ctsk* (Ambion, ThermoFisher Scientific; Cat#4457308) using Invivofectamine 3.0 (Ambion, ThermoFisher Scientific) following manufacturer's protocol - 1.2mg/mL of *Ctsk* siRNA solution was delivered via retro-orbital injection. Offspring were collected at E18.5 to confirm knockdown of *Ctsk* and osteoclast activity.

Mice carrying the $Ctsk^{Cre}$ (28) and $ROSA26^{DTA176}$ (29) alleles were mated to generate $Ctsk^{Cre}$;$DTA^{fl/+}$ offspring. *Ctsk* is expressed primarily in osteoclasts and would trigger the expression of Cre recombinase, which in turn would lead to expression of diphtheria toxin A (DTA), a bacteriophage exotoxin toxic to cells, and in this case, osteoclasts. $Ctsk^{Cre}$- or $ROSA26^{DTA176}$-null littermates were used as controls. Offspring were collected at E18.5 to analyze osteoclast activity.

Mice were sacrificed by CO_2 inhalation and fixed in 4% paraformaldehyde at 4ºC for 16-48h. Six-week old mice were collected and geometric morphometric analysis performed. For siRNA experiments, control (n=11) and experimental (n=15) mice were collected; for genetic experiments, control $Ctsk^{Cre}$;$DTA^{+/+}$ (n=15) and mutant $Ctsk^{Cre}$;$DTA^{fl/+}$ (n=10) mice were collected.

Quantitative PCR confirmation of Ctsk knockdown

Total RNA was isolated from E18.5 embryonic limbs injected with siRNA using the RNeasy kit (Qiagen). DNA was removed in-column with RNase-free DNAse

(Qiagen). qPCR reactions were performed using the GoTaq qPCR Master Mix (Promega) in a Mastercycler Realplex (Eppendorf). Prime-Time Primers (Integrated DNA Technologies, IDT) were utilized for qPCR (*Ctsk*, Mm.PT.58.10366461). qPCR conditions were as follows: 95°C, 2 min; 40 cycles at 95°C, 15 s; 58°C,15 s; 68°C, 20 s; followed by a melting curve gradient. Expression levels of the genes of interest were normalized to levels of *Rpl19*.

TRAP staining

Fixed E18.5 specimens were demineralized in 0.5M EDTA for 2 days, dehydrated, embedded in paraffin wax, and serially sectioned at 7μm. Ten equivalent sections spanning 70μm of the control and experimental mandible were analyzed. TRAP staining was performed using the Acid Phosphatase, Leukocyte Kit according to manufacturer's instructions (Sigma-Aldrich).

Micro-computed X-ray tomography (microCT)

Fixed 6-week old mouse heads were imaged at the Small ANimal Tomographic Analysis (SANTA) facility located at the Seattle Children's Research Institute using a Skyscan 1076 Micro-Computed Tomograph. Scans were performed at an isotropic resolution of 17.21m using the following settings: 55kV, 179A, 0.5mm Aluminum filter, 460ms exposure, rotation step of 0.7^{o}, 180° scan, and 3 frame averaging. All data were reconstructed using Nrecon (Version 1.6.9.4) with the same greyscale threshold. Reconstructions were converted to 3D volumes using Drishti v2.4 (30).

Morphometric data collection

Mandibles and skulls segmentations were performed with Avizo Lite (v 9.1.1). To quantify 3D shape and size variation of the skull and mandible between control and experimental mice, we characterized the craniofacial morphology using 3D landmark coordinates. Two sets of landmarks were defined: Set 1 included 13 paired bilateral landmarks that characterized the morphology of the mandible; Set 2 included 43 landmarks that characterized the morphology of the skull (Fig. S1).

Statistical Analysis

For qPCR and TRAP assays, the student t-test was used to determine significance. For 3D geometric morphometric analysis (GMA), landmark coordinates were exported as text files and imported to MorphoJ software to perform statistical shape analysis (31). First, mean forms for each group were calculated and superimposed using generalized Procrustes analysis to remove information about location and orientation, and scale all specimens by centroid size (defined as the square root of the sum of squared distances of each landmark coordinate from the mean x, y, z, landmark for the configuration or centroid). We computed the centroid size as a measure of overall size of the mandible and skull. Second, shape variation between control and experimental mice was analyzed by principal components analysis (PCA) and canonical variates analysis (CVA). PCA simplifies the dimensionality of data variation amongst individuals by reducing the data into a smaller number of orthogonal dimensions, whereas CVA identifies shape features that maximize the separation between control and experimental mice.

To determine whether allometry or size influenced shape variation between groups, we conducted multivariate regression of the Procrustes coordinates on centroid

size. The predicted values were then used as shape variables accounting for the allometric component of shape variation, and the residuals were used to investigate the shape variation independent of size, that is, the non-allometric component. Descriptive statistics were calculated for centroid size. The data followed a normal distribution, and thus numerical data were represented as the mean ± the standard deviation and compared by independent samples t-test using RStudio (v1.1.419) (http://www.R-project.org/). To determine interobserver reproducibility, two observers (MGH and RV) independently landmarked 10 randomly selected samples. A 1000 round permutation test was performed on Procrustes distances between the two observers' landmarks to determine overall shape differences.

Results

In vivo siRNA inhibition of Ctsk

We inhibited *Ctsk* using *in vivo* siRNA injected into E12.5 pregnant dams (Fig. 1A). Downregulation of *Ctsk* was confirmed by qPCR at E18.5 (Fig. 1B). Osteoclast activity was also confirmed to be decreased in E18.5 experimental animals (i.e., siRNA) compared to controls evidenced by TRAP staining (Fig. 1C-E).

We performed GMA on 6-week old mouse heads using landmarks of the skull and mandible (Fig. S1). Multivariate regression of shape on centroid size revealed that 31.7% and 16% of shape variation of experimental mandibles and skulls, respectively was due to static allometry or size differences compared to controls (data not shown). To analyze purely shape differences of the mandible and skull, we eliminated sources of allometry by using the residual values to perform principal components analysis (PCA) (Fig. 1F,G). We noted distinct clusters between control and experimental mandibles with some overlap, whereas control and experimental skulls showed increased overlap.

Canonical variate analysis (CVA) was performed to further analyze and determine shape changes associated with our landmarks (Fig. 2). Canonical variate 1 (CV1) showed distinct separation between control and experimental mandibles (Fig. 2A) and skulls (Fig. 2C). In the mandible, a decrease in osteoclast activity *in utero* was associated with a (i) lengthening of the adult mandibular body and (ii) shortening of the ramus height (Fig. 2B). We did not detect differences in the remainder of the experimental skull relative to controls (Fig. 2D).

Genetically modified alteration of osteoclast activity

We attempted to decrease osteoclast activity by generating *Ctsk*^{Cre};DTA$^{fl/+}$ mutant mice (Fig. 3A). In these mice, Cre recombinase is expressed under the control of the *Ctsk* promoter (e.g., osteoclasts), and activates expression of DTA. Surprisingly, instead of a decrease in TRAP activity in *Ctsk*^{Cre};DTA$^{fl/+}$ mutant mice, we observed an increase (Fig. 3B-D). This was similar to what was observed in a prior study where osteoclasts were attempted to be eliminated in *Ctsk*-inactivated mice (32). Instead of the expected reduction in osteoclast number, an increase in osteoclasts along with increased bone volume, bone formation rate, and osteoblast number were observed. Furthermore, *Ctsk*^{Cre} mice have previously been shown to lead to unintended consequences due to off-target events (33). Notably, homozygous expression of DTA (i.e., *Ctsk*^{Cre};DTA$^{fl/fl}$) led to embryonic lethality (data not shown).

Multivariate regression analysis of shape on centroid size revealed that 27.8% and 30.4% of the shape variation within mandible and skull datasets, respectively were due to static allometry (data not shown). We removed the influence of size differences to observe purely shape changes as described above. PCA showed distinct clusters of control (*Ctsk*^{Cre};DTA$^{+/+}$) and mutant (*Ctsk*^{Cre};DTA$^{fl/+}$) mandibles and skulls differing in PC1 (Fig. 3E,F).

To associate shape changes with our landmarks, we further performed CVA on mandibles and skulls (Fig. 4A,C). Separation between control and mutant mandibles and skulls was noted with CV1. In the mandible, an increase in osteoclast activity *in utero* was associated with (i) a decrease in mandibular body length and (ii) shortened ramus height (Fig. 4B). Furthermore, experimental mandibles also showed decreases in transverse width at the (i) condyle and (ii) gonion levels in dorsal views (Fig. 4B). In the

skull, an increase in osteoclast activity was associated with a shortening of (i) cranial and (ii) maxilla heights (Fig. 4D). However, experimental skulls showed an increase in (i) cranial width in dorsal view (Fig. 4D).

Discussion

Altering osteoclasts *in utero* led to changes in 6-week old mouse skulls - a decrease in osteoclast activity was associated with a lengthening of the adult mouse mandibular body (Fig. 1,2), whereas an increase in osteoclast activity was associated with a shortening of the mandibular body (Fig. 3,4), amongst other changes. These results support the findings first demonstrated in avian beak lengths (15).

Ctsk is a member of the papain-like cysteine protease family of genes expressed highly in osteoclasts to degrade type I collagen, osteopontin, and other bone matrix proteins rather than demineralization of the extracellular matrix (Alfaqeeh et al., 2015; Xue et al., 2014; Yamashita and Dodds, 2000; (34). Mutations in *CTSK* cause a rare autosomal recessive bone disorder called pycnodysostosis (OMIM 265800) with typical features including increased bone density, short stature, osteolysis of the distal phalanges, frequent pathologic fractures (16). Interestingly, osteoclasts are present before craniofacial mineralization (15) and during early and late tooth germ formation (35,36) highlighting yet unclear roles of *Ctsk* and osteoclasts beyond bone resorption and involvement in tooth eruption.

Inhibition of *Ctsk* and decreased osteoclast activity was confirmed at E18.5 via *in vivo* siRNA injection at E12.5 (Fig. 1A-E). The *in vivo* siRNA system can inhibit genes after 24h and upto a duration of 3 weeks although these times are gene-specific. Further experiments are required to catalog the efficacy and duration of inhibition after injection. Regardless, the observation that transient downregulation of *Ctsk* and osteoclast activity at specific stages in development can lead to changes in adult

mandibular morphology is surprising and novel. The implications of this observation are further discussed below.

We attempted to reduce osteoclast activity genetically using *Ctsk*^{Cre};DTA$^{fl/+}$ mice. Unexpectedly, we noted an increase in osteoclast activity (Fig. 3), a phenomena with some precedence (32,33). Whereas siRNA inhibition of *Ctsk* was transient, any cell expressing Cre recombinase and DTA under the *Ctsk* promoter would be globally and continuously eliminated. Thus, yet unclear compensatory mechanisms appear to have been triggered in *Ctsk*^{Cre};DTA$^{fl/+}$ mice, perhaps not surprising considering the complex coupling of bone formation and resorption (19) and wide expression profile of *Ctsk* (20,36). Regardless of these compensatory mechanisms, we serendipitously discovered that an increase in osteoclast activity was associated with shortening of the mandibular body.

With the loss of osteoclasts, *Rankl*$^{-/-}$ and *Rankl*$^{+/-}$ mice exhibited osteopetrosis with what appeared to be mandibular retrognathism (37), supporting our observation that osteoclast activity affects adult mandibular lengths. Moreover, associations between brachygnathia superior ("underbite" or Class III malocclusion) or brachygnathia inferior (Class II malocclusion) with osteopetrosis in wildlife has been noted previously (18,38). Even though mandibular retrognathism in *Rankl*-null mice is the opposite of what we observed in our study, it must be noted that *Rankl*$^{-/-}$ mice are devoid of any and all osteoclasts and *Rankl*-null mice have fewer or no osteoclasts throughout development making it difficult for comparison with our experiments. We are in the process of acquiring *Rankl*$^{f/f}$ mice (38) so that we may conditionally inactivate *Rankl* and osteoclasts during development.

Clearly bone modeling is a complex issue. Changes in osteoclast activity leads to changes in osteoblast activity and vice versa (19,39). Despite further studies that are required to dissect the downstream sequelae of altering osteoclast activity, our results suggest that altering osteoclast activity during critical developmental periods (e.g., before mineralization of offspring craniofacial bones) can lead to changes in adult jaw morphology and development of skeletal malocclusions. Notably, there are numerous reports of agents regulating osteoclast activity. For example, an organic compound called cyanidin is a pigment found in many berries including blueberry, cherry, cranberry, açai berry and raspberry that possesses inhibitory effects on osteoclastogenesis (40-43). We hypothesize that the intake of dietary factors during specific stages of pregnancy, such as cyanidin may alter osteoclast activity in offspring and contribute to changes in craniofacial morphology and the development of skeletal malocclusion. A better understanding of the biology of skeletal malocclusions especially at the molecular and cellular levels is a prerequisite for potential advances in their diagnosis and prevention.

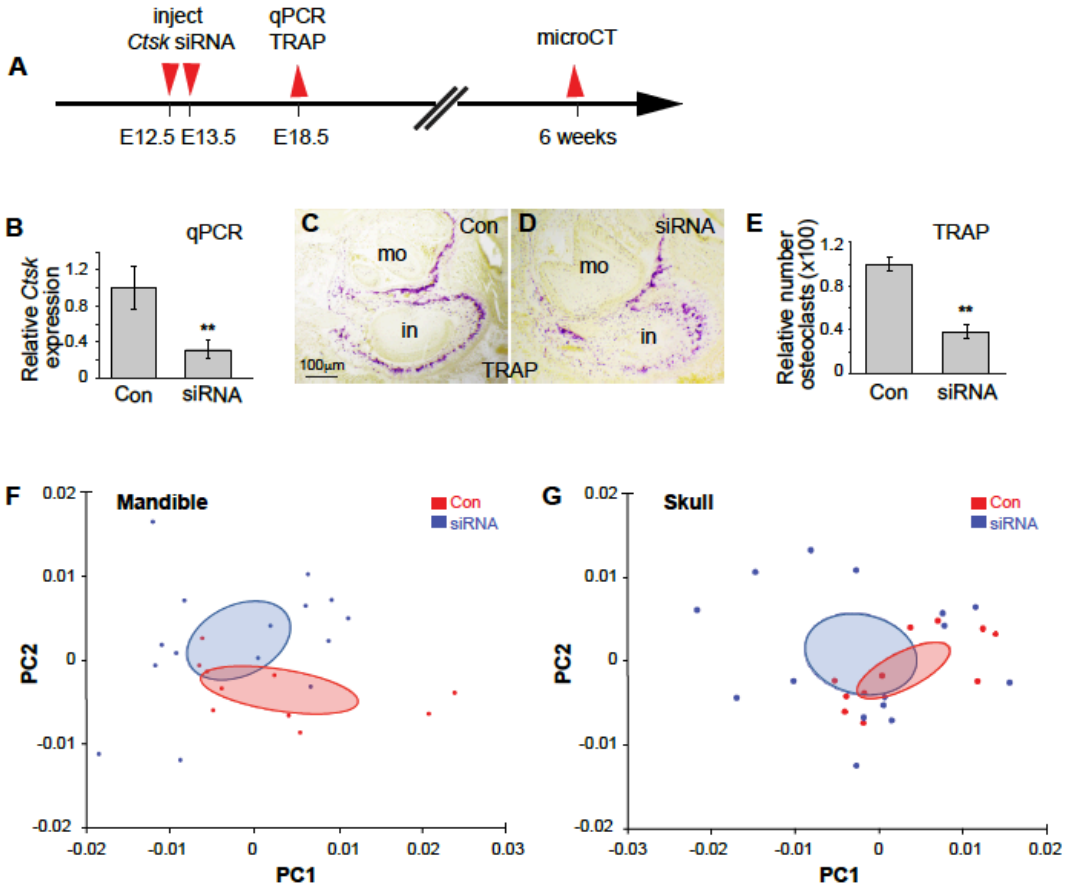

Fig. 2.1 *In vivo* siRNA knockdown of *Ctsk in utero* leads to changes in osteoclast activity and 3D morphological differences. (A) Experimental design. (B) Confirmation of *Ctsk* downregulation by *in vivo* siRNA. (C-E) Confirmation of decreased TRAP activity in control and experimental mice. (F,G) PCA for control and experimental mandible (F) and skull (G).

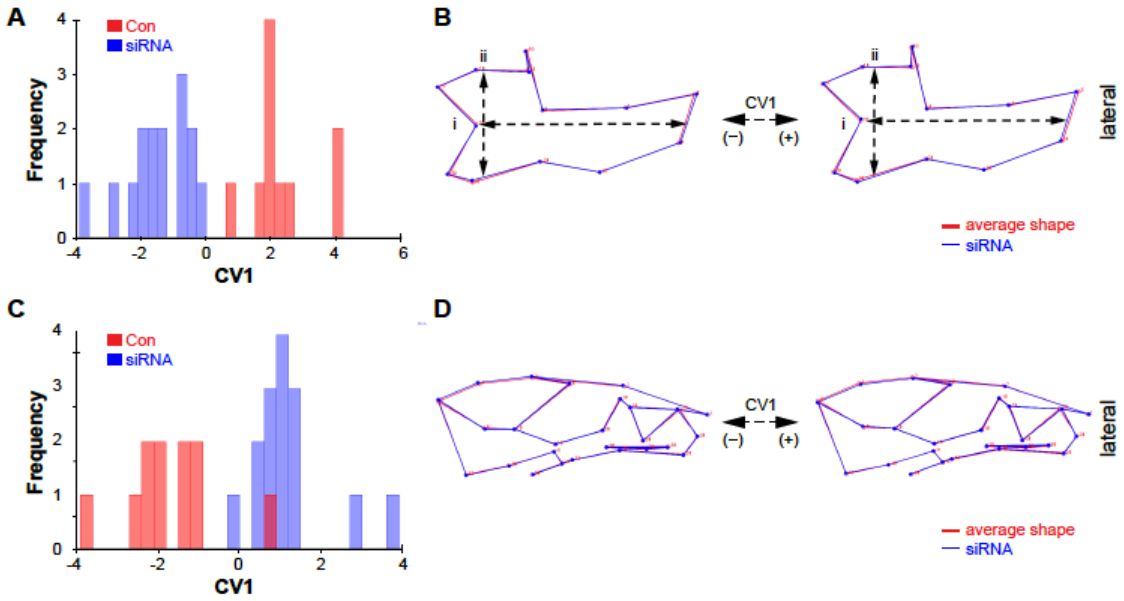

Fig. 2.2 *In vivo* siRNA knockdown of *Ctsk in utero* is associated with a lengthening of the mandibular body using geometric morphometrics analysis. (A,C) CVA shows clear separation between control and experimental CV1 in mandible (A) and skull (C). (B,D) Wireframe illustrations representing changes in mandible (B) and skull (D) with positive/negative CV1 values.

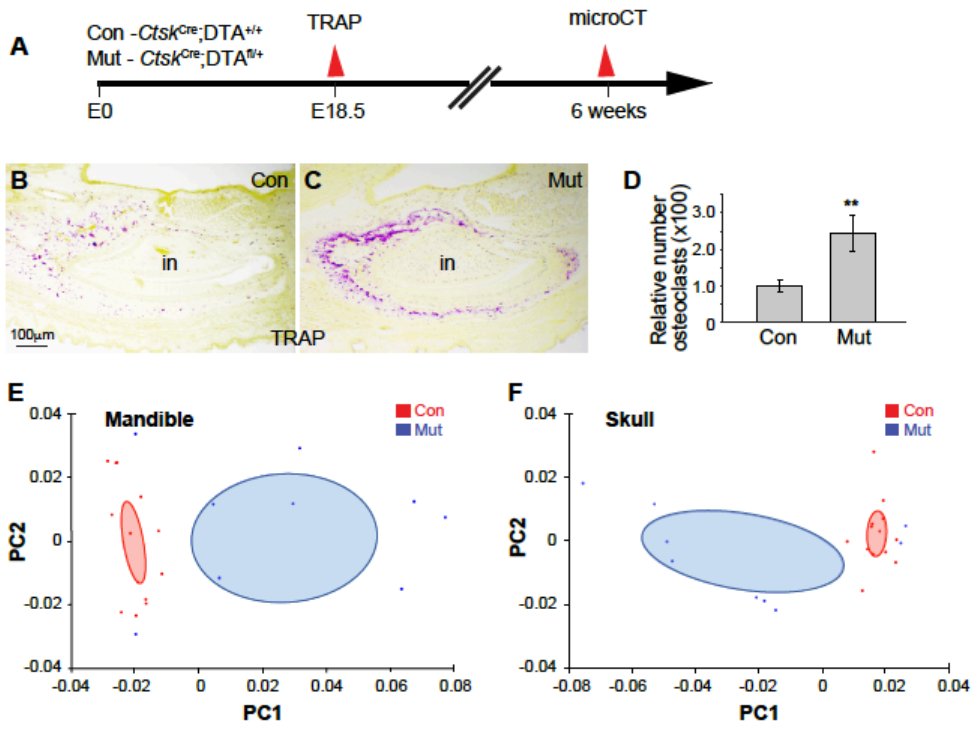

Fig. 2.3 *Ctsk*^{Cre};DTA$^{fl/+}$ mutant mice show an increase in osteoclast activity and 3D morphological differences. (A) Experimental design. (B-D) Confirmation of decreased TRAP activity in control (*Ctsk*^{Cre};DTA$^{+/+}$) and mutant (*Ctsk*^{Cre};DTA$^{fl/+}$) mice. (E,F) PCA for control and mutant mandible (E) and skull (F).

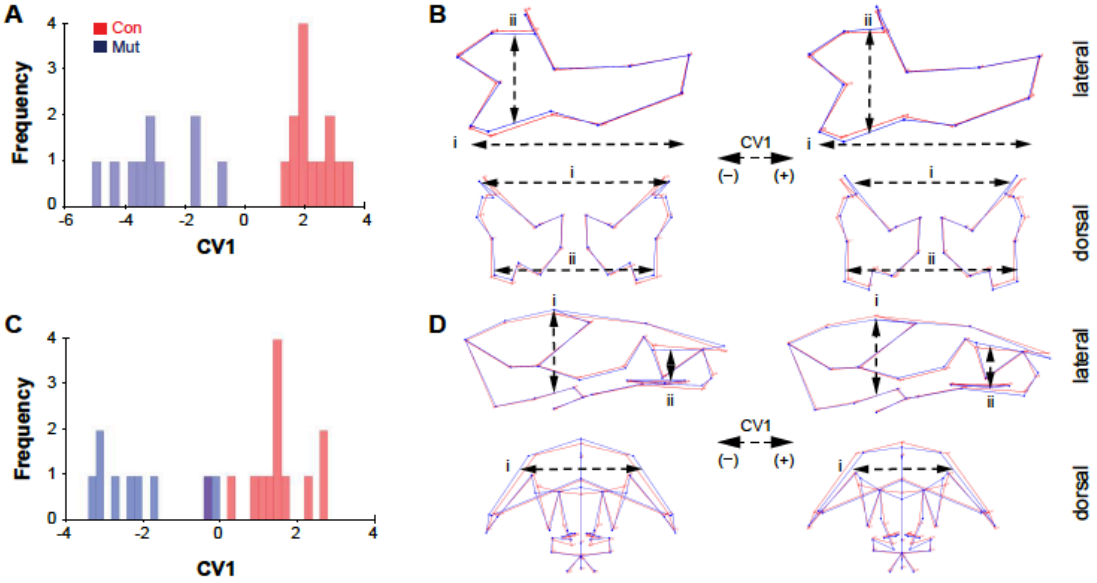

Fig. 2.4 An increase in osteoclast activity in *Ctsk*^{Cre};DTA$^{fl/+}$ mutant mice is associated with a shortening of the mandibular body using geometric morphometrics analysis. (A,C) CVA shows clear separation between control and mutant CV1 in mandible (A) and skull (C). (B,D) Wireframe illustrations representing changes in mandible (B) and skull (D) with positive/negative CV1 values.

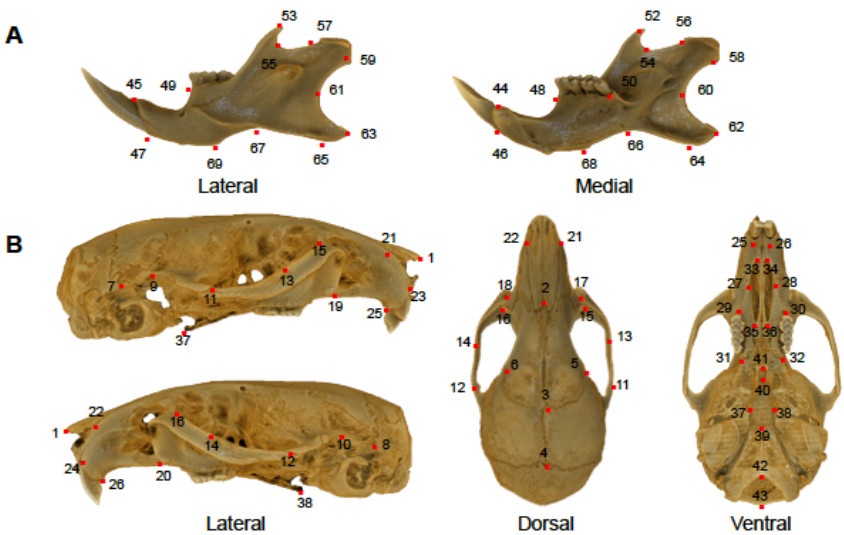

C

Landmark	Description
1	Nasal bone's most anterior suture
2	Nasal bone's most posterior suture
3	Frontal bone's most posterior suture
4	Parietal bone's most posterior suture
5-6	Frontal-squasmosal intersection at temporal crest
7-8	The intersection between parietal, occipital and squamosal bones
9-10	Joining of squasmosal body to zygomatic process
11-12	Most anterior suture of jugal bone and the maxillary zygomatic process
13-14	Mid zygomatic bone
15-16	Intersection of frontal process of maxilla with frontal and lacrimal bones
17-18	
19-20	
21-22	Anterior-most point at intersection of premaxillae and nasal bones
23-24	Most superior point of the incisor alveolus
25-26	Most inferior anterior point of the incisor alveolus
27-28	Most inferior lateral point on premaxilla-maxilla suture
29-30	Most anterior point of the first molar alveolus
31-32	Most posterior point of the third molar alveolus
33-34	Most anterior point of the anterior palatine foramen
35-36	Most posterior point of the anterior palatine foramen
37-38	Most inferior aspect of posterior tip of medial pterygoid process
39	Line point of the suture between occipital and basisphenoid bones
40	Line point of the suture between basisphenoid and presphenoid bones
41	Line point of the suture between palatine bones.
42	Foramen magnum most anterior point, basion
43	foramen magnum most posterior point, bregma
44-45	Most superior point of incisor alveolus
46-47	Most inferior point of the incisor alveolus
48-49	Most anterior point of the first molar alveolus
50-51	Most posterior point of the third molar alveolus
52-53	Most posterior tip of the coronoid process
54-55	Most anterior/inferior concave point of the left coronoid process
56-57	Most anterior point of the articular surface of the condyle
58-59	Most posterior tip of the condyle
60-61	Most anterior concave point between condyle and angle of the mandible
62-63	Most posterior tip of the mandibular angle
64-65	Most inferior point of the mandibular angle
66-67	Ascending ramus dorsal-most ventral point
68-69	Most inferior point of alveolar region

Figure 2.5 Landmarks of Mouse Skull

Chapter 3:

Altering calcium and phosphorus levels in utero affects adult mouse mandibular morphology

The purpose of our study was to determine morphological changes in the adult mandible of offspring exposed to high calcium, low phosphorus diets in utero until weaning age. Time-mated FVB wildtype mice were fed normal or experimental diet during gestation and until weaning of offspring. Experimental diet contained 3-fold increase in calcium and 3-fold decrease in phosphorus compared to normal diet. Six-week old offspring were sacrificed and heads scanned using micro-computed tomography. Three-dimensional geometric morphometric analysis was utilized to detect morphological changes to the mandible including the condyle. Experimental females showed the greatest morphological differences including shortened mandibular ramus width and height, shortened mandibular body length and height, a wider but shortened condylar neck, and a wider condylar head in the lateral-medial direction. Experimental male mandibles trended towards increased mandibular body height and length, opposite the changes observed in experimental female mandibles, whereas condyles were similar to that observed in experimental females. Bone mineral density (BMD) was decreased in experimental females. Increased calcium and decreased phosphorus levels in utero led to a retrognathic mandible associated with lowered BMD in experimental females, whereas experimental males showed partly opposite effects. Further studies are required to understand the mechanism underlying diet- and gender-specific differences in mandibular morphology

Introduction

In 1899, Edward H. Angle classified malocclusions as Class I, II, and III based on maxillary and mandibular permanent molar relationships (1). Class II and Class III skeletal malocclusions are a result of discrepancies in the morphology of the maxilla and/or mandible, and treatment often requires extractions and/or orthognathic surgery leading to increased overall treatment and chair time. Prevalence of Class II and Class III malocclusions in Caucasian populations have been reported to be 23% and 3.4% respectively (3), whereas Class III malocclusions in Asian populations ranges from 10-16% (2). The etiology of skeletal malocclusion is yet unclear. In the 19th century, skeletal malocclusions were theorized to be caused by dietary deficiencies, endocrine malfunction, or mental degeneracy rather than genetic transmission (4). However, the relationship between genetics and skeletal malocclusion has been cemented began to gain momentum since the 1960's (4,5), which ultimately resulted in the identification of several candidate genes that play a role in the etiology of Class II and Class III malocclusion. For example, collagen type 1A (COLIAI), cartilage matrix protein matrilin-1 (MATN1), and fibroblast growth factor 2 (FGFR2) were associated with increased risk of Class III malocclusion, whereas T-Box 5 (TBX5) was associated with decreased risk (8). Perillo et al. (2015) used wholeexome sequencing to analyze the genetic composition of a family with 30% of its members displaying Class III malocclusions - a G1121S variant of Rho GTPase Activating Protein 21 (ARHGAP21) was present in all prognathic family members (9). Ikuno et al. (2014) identified two chromosome regions (1q32.2 and 1p22.3) likely to be susceptible regions of mandibular prognathism - Plexin A2 (PLXNA2) and Synovial Sarcoma, X Breakpoint 2 Interacting Protein (SSX2IP),

neither of which were previously linked to craniofacial growth were closely associated with these two regions (10). Despite examples of putative candidate genes involved in skeletal malocclusions, environmental factors (excluding trauma and pathologies) also likely play an important role in skeletal malocclusions (44). Prior experiments showed that inhibiting osteoclast activity during quail embryogenesis led to increases in lower beak lengths (15). Bone-resorbing osteoclasts are sensitive to calcium and phosphorus levels. For example, excessive calcium levels can impair growth and bone mineralization due to reduced efficacy of phosphorus absorption, (23) whereas phosphorus deficiency led to increased osteoclast size and number (24). The purpose of this study was to determine whether a maternal diet of excess calcium and phosphorus deficiency during gestation until weaning age would lead to three-dimensional (3D) morphological changes in adult offspring mandibles. We hypothesized that our experimental diet would result in mandibular retrognathism due to increased osteoclast activity. We noted both diet- and gender-specific morphological changes in the mandible.

Material and Methods

Animals

Breeding pairs of FVB mice (Jackson laboratory) and offspring upto 3 weeks of age were fed either a normal or experimental diet. Normal (#58M1, LabDiet, St. Louis Missouri, USA) and experimental (#5BLX, LabDiet) diet were identical except that the experimental diet contained a 3-fold increase in calcium and 3-fold decrease in phosphorus. Food and water were available ad libitum. Mice were housed under a 12/12-h light-dark cycle at a constant temperature of 22±1°C and humidity of 50±5%. At weaning, all mice were fed normal diet (from 3 to 6 weeks). Eleven control offspring (6 females; 5 males) and 10 experimental offspring (6 females; 4 males) from 3 pregnant mice in each cohort were weighed and sacrificed at 6-weeks of age. Mouse heads were fixed in 4% paraformaldehyde at 4ºC for 48h. All aspects of animal care and experiments were approved by the Institutional Animal Care and Use Committee (IACUC) at UCSF and performed under animal research protocol number AN164201. Micro-computed Tomography and Segmentation Fixed mouse heads were subjected to micro-computed tomography (microCT) using a SkyScan 1076 MicroCT at the Small Animal Tomographic Analysis Facility (SANTA) located at Seattle Children's Research Institute. Specimens were scanned at 17.2 micron resolution (55 kV, 150 mA, 0.5 mm Al filter). Reconstructions were generated using NRecon (Version 1.6.9.4) with consistent thresholding parameters, converted to 3D volumes, and visualized using Drishti (version 2.6) (30). Mandibular segmentations from microCT data were performed with Avizo Lite (version 9.1.1).

Morphometric Analysis

To quantify 3D shape and size variation of the mandible between control and experimental mice, we characterized mandibular morphology using 3D landmark coordinates. Two sets of landmarks were defined: set 1 included 26 bilateral landmarks that characterized the morphology of the mandible (Table 1A,C); Set 2 included 50 sliding semi-landmarks that were distributed across the right condyle of all specimens using Landmark software (Table 1B) (45). Nine of these points were placed along the condyle head and the external surface of the condylar neck until an imaginary line passing from the tip of the coronoid process to the gonial angle (i.e., tip of the mandibular angle). The landmarks were digitized by RV and revised by MGH. To assess measurements, a random subsample of 7 mice was used to test error in locating the landmarks and semi-landmarks between observers. Procrustes ANOVA was used to test the reliability of the observations.

Landmark coordinates were exported as text files and imported to MorphoJ software to perform statistical shape analyses (31). Briefly, mean forms for each group were calculated and superimposed using generalized procrustes analysis to remove information about location and orientation, and scale all specimens by centroid size (calculated as a measure of overall size of the mandible). Shape variation between control and experimental mandibles was analyzed by principal components analysis (PCA) and canonical variates analysis (CVA). PCA simplifies the dimensionality of data variation amongst individuals by reducing the data into a smaller number of orthogonal dimensions, whereas CVA identifies shape features that maximize the separation between control and experimental mice.

To determine whether allometry or size influenced shape variation between groups, we conducted multivariate regression of the Procrustes coordinates on centroid size. The predicted values were then used as shape variables accounting for the allometric component of shape variation, and the residuals were used to investigate the shape variation independent of size when necessary. The data followed a normal distribution, and thus numerical data were represented as the mean ± the standard deviation and compared by independent samples t-test using RStudio (version 1.1.419) (46).

Analysis of Bone Mineral Density

Bone mineral density (BMD) was measured from a region of interest sphere created within the mandibular ramus (Table 2) using CTAn software (version 1.17.7.2+, Bruker microCT) following calibration with commercially supplied calcium hydroxyapatite phantoms of known density (0.25-0.75 g/cm3). The area measured was located posteriorly to the mandibular incisor and at the widest portion of the ramus when visualized in the coronal plane. All measurements were blinded to intervention. Descriptive statistics were calculated for BMD. Independent-samples t-test was conducted to analyze the results using RStudio (version 1.1.419) (46).

Results

High calcium/low phosphorus diet leads to differences in mandibular morphology

Multivariate regression of shape on centroid size revealed that 29.4% of shape variation within the dataset was due to static allometry - size of experimental mandibles was smaller than controls (data not shown). Once the effects of allometry were removed by using the residuals to examine variation within the sample, we noted clustering of control and experimental mandible using PCA (Fig. 1A). Principal components 1 (PC1) accounted for 37.4% of total variance. Experimental mandibles tended to have lower/negative PC1 values (Fig. 1A). When male and female specimens were separated, gender-specific differences were observed (Fig. 1B). Control male/female and experimental male mandible were clustered similarly, whereas experimental females trended towards lower/negative PC1 values. Lower/negative PC1 values were associated with increased width/height of the ramus (i,iii), increased length between the gonial angle and the most inferior point of the incisor alveolus (ii), and increased height of the body (iv) (Fig. 1C).

Condyle

Multivariate regression of shape based on centroid size revealed that 11.9% of condylar shape variation was due to static allometry - size was not significantly affecting shape variation (data not shown). Regardless, size correction was performed as described above. Distinct clusters were observed between control and experimental condyles (Fig. 2A). Gender-specific differences were also observed in condylar morphology with experimental females trending to lower/negative PC1 values and

experimental males trending towards lower/negative PC2 values compared to their respective controls (Fig. 2). PC1 and PC2 were responsible for 31.1% and 22.5% respectively, of the total variance and procrustes ANOVA indicated significant shape differences between clusters (Pvalue < 0.0001). Lower/negative values of PC1 were associated with a wider condylar neck due to increased anterior width (i) and shortened neck height (ii), whereas lower/negative PC2 values were associated with a wider condylar neck due to increase posterior width (i) and shortened neck height (ii) (Fig. 2C). In addition, lower/negative PC1 and PC2 values appeared to be associated with condylar heads that were more oval in shape (data not shown).

CVA of Mandible Including Condyle

CVA confirmed significant differences between the mean shape configurations of control and experimental mandibles including condyles based on gender and diet (Fig. 3). CVA generated distinct clustering patterns with male and female controls showing the most overlap for mandibles (Fig. 3A) and condyles (Fig. 3C). Experimental female mandibles showed lower/negative CV1 and CV2 values, whereas experimental male mandibles showed higher/positive CV2 values (Fig. 3A). Experimental female condyles showed higher/positive CV1 values, whereas experimental male condyles showed lower/negative CV2 values (Fig. 3C). For mandibles, lower/negative CV1 values were associated with decreased ramus height (i), decreased ramus width (ii), and shortened body length (iii), whereas higher/positive CV2 values were associated with increased body height (i) (Fig. 3B). For condyles, higher/positive CV1 values were associated with increased condylar neck width (i) and decreased neck height (ii) in lateral views, and

increased condylar head lateral-medial widths leading to more oval-shaped heads (i) in anterior-posterior (an-po) views, whereas lower/negative CV2 values were associated with increased posterior neck width (i) (Fig. 3D).

BMD

To determine whether BMD was affected by the elevated calcium and phosphorus-deficient diet, BMDs of offspring adult mandibles were measured. Control mice exhibited significantly greater mandibular bone density than experimental mice (Table 2). Interestingly, this difference was mainly due to the significantly lower BMD of experimental female mandibles, whereas experimental male mandibles showed no BMD differences.

Discussion

Environmental factors during development play an important role in craniofacial skeletal abnormalities and malocclusion. However, the roles of shifting calcium and phosphorus levels in utero on mandibular morphology and malocclusion are unknown. Calcium and phosphorus concentrations in fetal serum significantly exceed the normal range in healthy, non-pregnant adult (47). Although the demand for additional calcium during pregnancy is recognized, the dietary reference intake for calcium was lowered for pregnant women in 1997 to amounts recommended for non-pregnant women (48), due to fears of hypercalcemia or increase calcium concentration of calcium that may lead to hyperparathyroidism, lung diseases, dehydration, medication side effects, and/or dietary supplements (49-52).

In our present study, we found that a high calcium, low phosphorus diet during pregnancy altered the morphology of offspring adult mandibles. Routinely, two-dimensional (2D) cranio- and cephalo-metrics are utilized in orthodontics to measure size, proportions, and relationships between facial structures, but threedimensional (3D) analysis provides a more detailed, efficient, and accurate method (53,54). Using 3D GMA of adult offspring exposed to experimental food during gestation until weaning, we noted distinct morphological changes to the mandible including condyles. Furthermore, we noted gender-specific differences. Both finding are novel and lead to numerous questions regarding environment and skeletal malocclusion.

Experimental females showed the greatest morphological differences presenting with shortened mandibular ramus width and height, as well as shortened mandibular body length and height (Fig. 3B). Experimental female condyles showed a wider but

shortened neck with a wider condylar head in the lateral-medial direction (Fig. 3D). Together with lowered BMDs (Table 2), which is correlated with an increase in osteoclast activity, the changes observed in experimental females confirm our hypothesis that high calcium, low phosphorus diets will lead to decreased osteoclast activity resulting in retrognathic mandibles. To reiterate, our hypothesis was based on prior studies showing the amount of bone resorption in developing birds is inversely proportional to jaw length (15).

Experimental male mandibles trended towards increased body height and potentially length based on CV2 values (Fig. 3B), opposite the changes observed in experimental female mandibles. Experimental male condylar necks were wider similar to that observed in experimental females (Fig. 3D). We noted that there was little or no BMD changes in males suggesting that calcium and phosphorus levels may not affect males to the extent observed in females. Such gender differences associated with in utero diet modification have yet to be documented. Further experiments are required to better understand gender-specific effects on mandibular morphology due to calcium and phosphorus changes in utero.

The effects of maternal calcium intake during gestation on offspring bone are unclear. Several studies showed a positive relationship between maternal calcium intake and offspring bone outcomes (55,56), yet other studies have reported inconsistent results (57,58). However, maternal hypercalcemia has been shown to cause late neonatal hypocalcemia (59, 60). It is possible that maternal hypercalcemia affects mandibular morphogenesis indirectly by increasing offspring osteoclast count in response to neonatal hypocalcemia.

Post-pubertal hypercalcemia may reduce muscle strength and function, (61) and a reduction of masticatory muscles function decreases mandibular size (62,63). The offspring in our study were exposed to experimental diet throughout pregnancy and continued from birth until weaning (newborn to 3-week old). Our future study will not expose offspring after birth to delineate specific in utero effects. The increased calcium intake might also have an effect on the function and strength of masticatory muscles, especially since we noted shape changes in muscle insertion sites such as the mandibular condyle, ramus, and the gonial angle. Furthermore, future studies will include evaluation of maternal and offspring calcium/phosphorus serum levels.

Conclusion

Our results demonstrate that altering calcium and phosphorus levels in utero lead to morphological changes in adult offspring mandibles likely due to changes in bone turnover. Increased calcium and decreased phosphorus levels led to a retrognathic mandible associated with lowered BMD in experimental females, whereas experimental males showed opposite effects. Further studies are required to understand the mechanism underlying diet- and gender-specific differences in mandibular morphology.

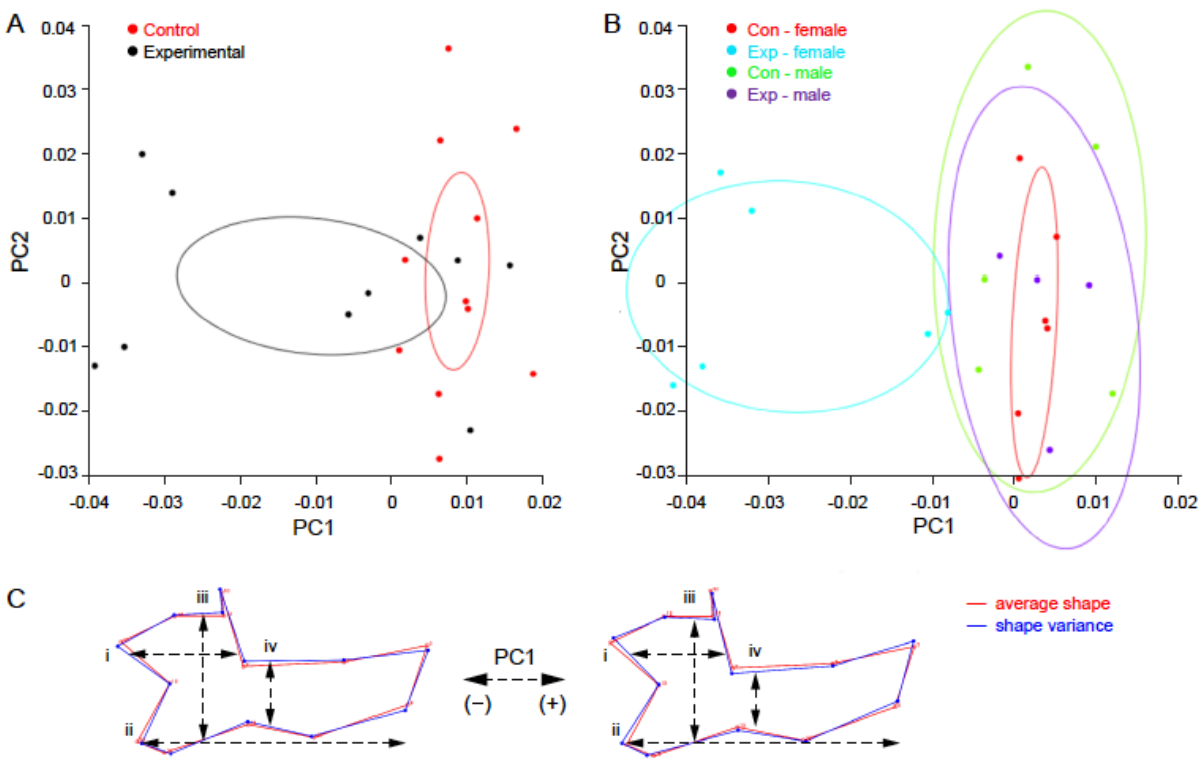

Fig. 3.1 Principal components analysis (PCA) of regression residuals of shape variation in the mandible. (A) Clusters representing shape differences based on PC1 and PC2 values. (B) Gender-specific shape differences. (3) Shape warps illustrate extreme examples of shape changes associated with positive/negative PC1 and PC2 values of the mandible in lateral view.

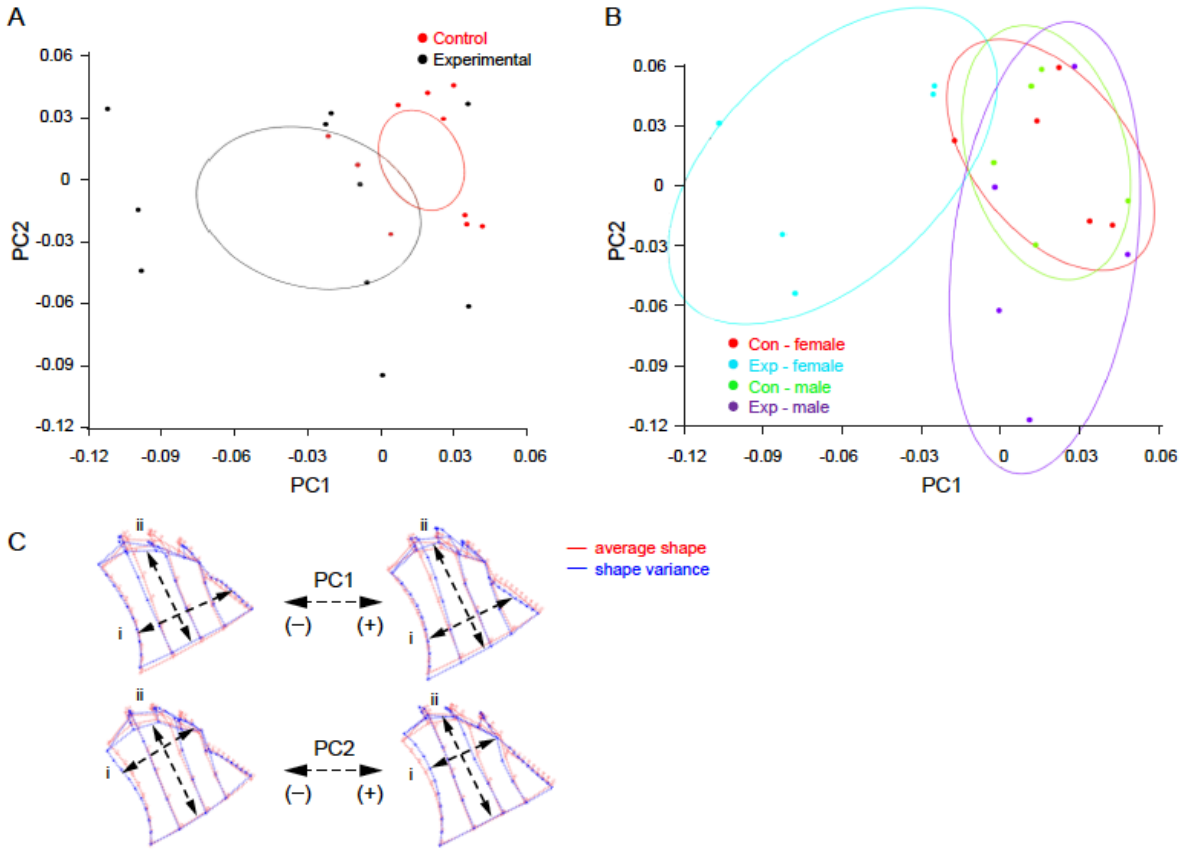

Fig. 3.2 Principal components analysis (PCA) of regression residuals of shape variation in the condyle. (A) Clusters representing shape differences based on PC1 and PC2 values. (B) Gender-specific shape differences. (3) Shape warps illustrate extreme examples of shape changes associated with positive/negative PC1 and PC2 values of the condyle in lateral view.

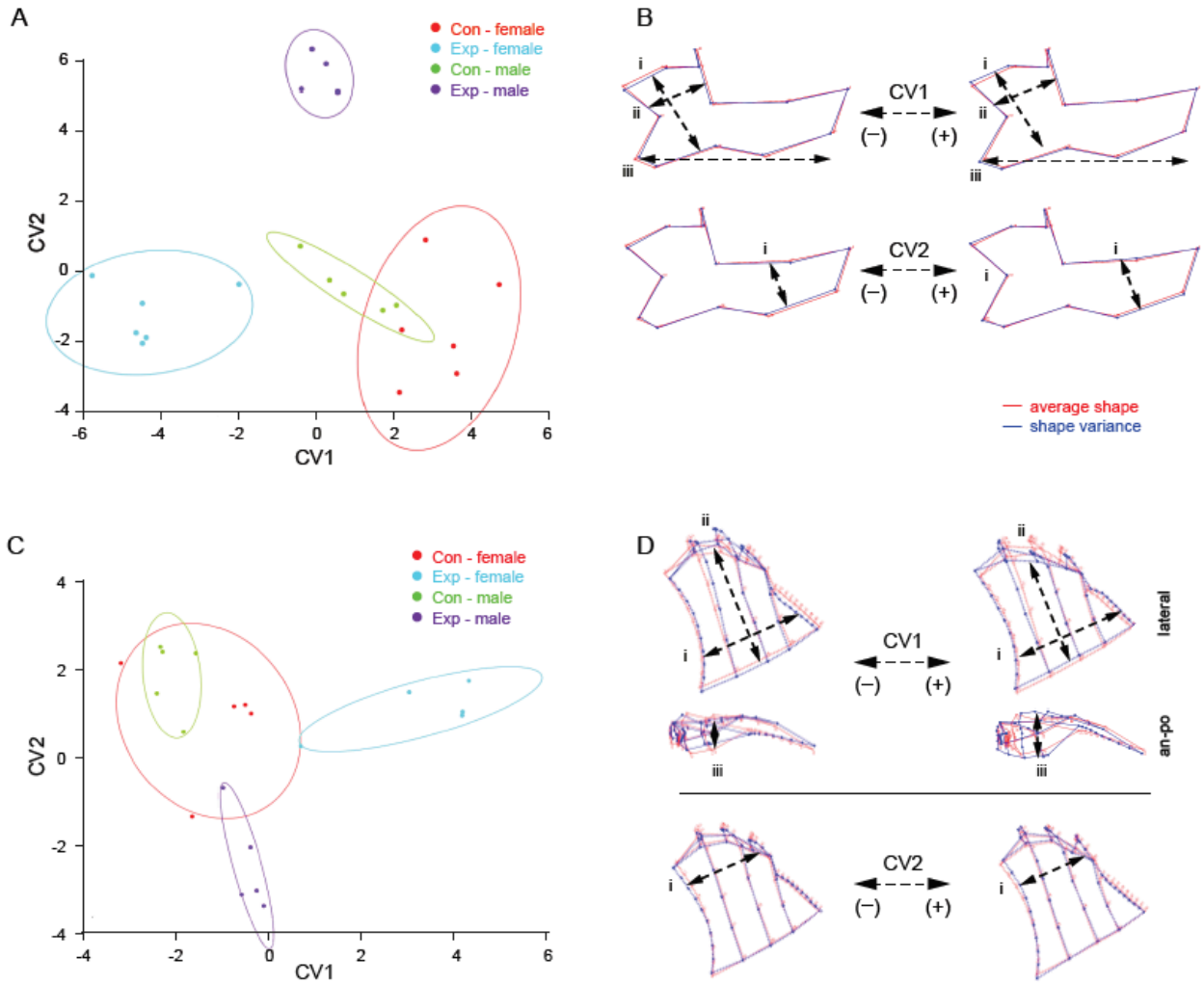

Fig. 3.3 Canonical variate analysis (CVA) of the mandibular condyles. (A) Shape differences for the mandible that are associated with CV1 and CV2 are shown for each group. (B) Shape warps illustrate extreme examples of shape changes associated with positive/negative CV1 and CV2 values of the mandible in lateral view. (C) Shape differences for the condyle. (D) Shape warps showing extreme shape changes associated with positive/negative CV1 and CV2 values of the condyle in lateral and anterior-posterior (an-po) views.

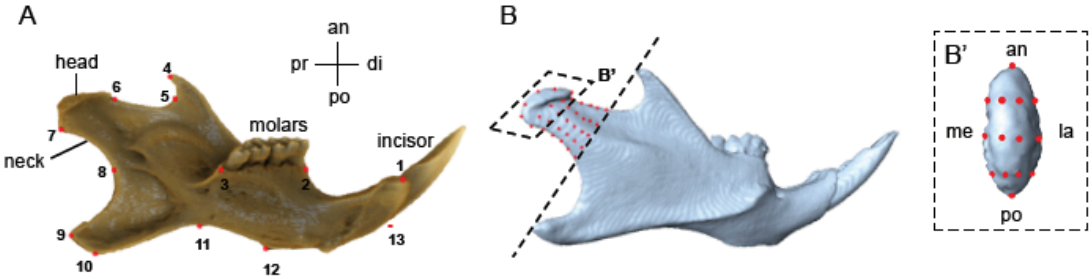

C

Landmark	Description
1	Most superior point of incisor alveolus
2	Most anterior point of the first molar alveolus
3	Most posterior point of the third molar alveolus
4	Most posterior tip of the coronoid process
5	Most anterior/inferior concave point of the left coronoid process
6	Most anterior point of the articular surface of the condyle
7	Most posterior tip of the condyle
8	Most anterior concave point between the condyle and the angle of mandible
9	Most posterior tip of the mandibular angle
10	Most inferior point of the mandibular angle
11	Ascending ramus dorsal-most ventral point
12	Most inferior point of alveolar region
13	Most inferior point of the incisor alveolus

Figure 3.4 Mouse mandible and landmarks. (A) Light micrograph image of the mouse right hemi-mandible in lateral view showing the condylar head and neck, three molars, and incisor. (B) A segmented hemi-mandible in lateral view showing landmarks (red dots) of the condylar head (black dashed box) and neck proximal to the set border (black dashed line). (B') Magnified proximal view of the condylar head. Red dots indicate all landmarks. an, anterior; di, distal; po, posterior; pr, proximal.

Table 3.1 Bone mineral density measurements.

Groups		Mean (g/cm3)	SD	P value
All	Control	1.15	0.11	0.05*
	Experimental	1.01	0.06	
Female	Control	1.19	0.12	0.004*
	Experimental	0.93	0.11	
Male	Control	1.10	0.07	0.91
	Experimental	1.08	0.24	

References

1. Angle EH. Classification of Malocclusion. *Dent Cosmos*1899;41:248-64.

2. Ngan P, Moon W. Evolution of Class III treatment in orthodontics. *Am. J. Orthod. Dentofacial Orthop.*2015;148(1):22-36. doi:10.1016/j.ajodo.2015.04.012.

3. Angle EH. *Treatment of Malocclusion of the Teeth and Fractures of the Maxillae*. 6th ed. Philadelphia: SS White Dental Mfg Co; 1900.

4. Carlson DS. Evolving concepts of heredity and genetics in orthodontics. *Am. J. Orthod. Dentofacial Orthop.*2015;148(6):922-938. doi:10.1016/j.ajodo.2015.09.012.

5. Nakasima A, Ichinose M, Nakata S, Takahama Y. Hereditary factors in the craniofacial morphology of Angle's Class II and Class III malocclusions.*Am. J. Orthod.*1982;82(2):150-156.

6. Otero LM, Morford LA, Falcao-Alencar G, Hartsfield JK. Family history and genetics of mandibular prognathism. Sharjah, United Arab Emirates: Bentham Science; 2014.

7. Nakasima A, Ichinose M, Nakata S, Takahama Y. Hereditary factors in the craniofacial morphology of Angle's Class II and Class III malocclusions. Am J Orthod 1982;82:150-156.

8. da Fontoura CSG, Miller SF, Wehby GL, et al. Candidate gene analyses of skeletal variation in malocclusion. *J. Dent. Res.*2015;94(7):913-920. doi:10.1177/0022034515581643.

9. Perillo L, Monsurrò A, Bonci E, Torella A, Mutarelli M, Nigro V. Genetic association of ARHGAP21 gene variant with mandibular prognathism. *J. Dent. Res.*2015;94(4):569-576. doi:10.1177/0022034515572190.

10. Ikuno K, Kajii TS, Oka A, Inoko H, Ishikawa H, Iida J. Microsatellite genome-wide association study for mandibular prognathism. *Am. J. Orthod. Dentofacial Orthop.*2014;145(6):757-762. doi:10.1016/j.ajodo.2014.01.022.

11. Larsen CS. The agricultural revolution as environmental catastrophe: Implications for health and lifestyle in the Holocene. Quaternary International. 2006 Jun;150(1):12–20.

12. Rando C, Hillson S, Antoine D. Changes in mandibular dimensions during the mediaeval to post-mediaeval transition in London: a possible response to decreased masticatory load. Arch Oral Biol 2014;59:73-81.

13. von Cramon-Taubadel N. Global human mandibular variation reflects differences in agricultural and hunter-gatherer subsistence strategies. Proc Natl Acad Sci USA. 2011 Dec 6;108(49):19546–51.

14. Zaidi M. Skeletal remodeling in health and disease. Nat Med. 2007 Jul;13(7):791–801.

15. Ealba EL, Jheon AH, Hall J, Curantz C, Butcher KD, Schneider RA. Neural crest mediated bone resorption is a determinant of species-specific jaw length. Dev Biol 2015;408:151-163.

16. Xue Y, Cai T, Shi S, Wang W, Zhang Y, Mao T, et al. Clinical and animal research findings in pycnodysostosis and gene mutations of cathepsin K from 1996 to 2011. Orphanet J Rare Dis. 2011 May 10;6:20.

17. Turk V, Turk B, Turk D. Lysosomal cysteine proteases: facts and opportunities. EMBO J. 2001;20(17):4629–4633. doi: 10.1093/emboj/20.17.4629.

18. Hoy JA, Haas GT, Hoy RD, Hallock P. Observations of brachygnathia superior (underbite) in wild ruminates in Western Montana, USA. Wildl Biol Pract. 2011 Sep 21;7(2).

19. Ikebuchi Y, Aoki S, Honma M, Hayashi M, Sugamori Y, Khan M, et al. Coupling of bone resorption and formation by RANKL reverse signalling. Nature. 2018 Sep 5;561(7722):195–200.

20. Podgorski I, Linebaugh BE, Koblinski JE, Rudy DL, Herroon MK, Olive MB, et al. Bone marrow-derived cathepsin K cleaves SPARC in bone metastasis. Am J Pathol. 2009 Sep;175(3):1255–69.

21. Dana, H., Chalbatani, G. M., Mahmoodzadeh, H., Karimloo, R., Rezaiean, O., Moradzadeh, A., … Gharagouzlo, E. (2017). Molecular Mechanisms and Biological Functions of siRNA. *International journal of biomedical science : IJBS*, *13*(2), 48–57.

22. Ryther RCC, Flynt AS, Phillips III JA, Patton JG. siRNA therapeutics: big potential from small RNAs. *Gene Ther*. 2004;12:5. https://doi.org/10.1038/sj.gt.3302356.

23. Zhu YW, Wen J, Jiang XX, Wang WC, Yang L. High calcium to phosphorus ratio impairs growth and bone mineralization in Pekin ducklings. Poult. Sci. 2018;97(4):1163 1169. doi:10.3382/ps/pex401.

24. Thompson ER, Baylink DJ, Wergedal JE. Increases in number and size of osteoclasts in response to calcium or phosphorus deficiency in the rat. Endocrinology 1975;97(2):283-289. doi:10.1210/endo-97-2-283.

25. Toro-Ibacache V, Ugarte F, Morales C, Eyquem A, Aguilera J, Astudillo W. Dental malocclusions are not just about small and weak bones: assessing the morphology of

the mandible with cross-section analysis and geometric morphometrics. *Clin Oral Investig*. January 2019. doi:10.1007/s00784-018-2766-6)

26. Dewey M. Classification of malocclusion. International Journal of Orthodontia. 1915 Mar;1(3):133–47.
27. Inaoka T, Bilbe G, Ishibashi O, Tezuka K, Kumegawa M, Kokubo T. Molecular cloning of human cDNA for cathepsin K: novel cysteine proteinase predominantly expressed in bone. Biochem Biophys Res Commun. 1995 Jan 5;206(1):89–96.
28. Chiu WSM, McManus JF, Notini AJ, Cassady AI, Zajac JD, Davey RA. Transgenic mice that express Cre recombinase in osteoclasts. Genesis. 2004 Jul;39(3):178–85.
29. Wu S, Wu Y, Capecchi MR. Motoneurons and oligodendrocytes are sequentially generated from neural stem cells but do not appear to share common lineage-restricted progenitors in vivo. Development. 2006 Feb;133(4):581–90.
30. Limaye A. Drishti: a volume exploration and presentation tool. Developments in X-Ray Tomography VIII. SPIE; 2012. p. 85060X.
31. Klingenberg CP. MorphoJ: an integrated software package for geometric morphometrics. Mol Ecol Resour. 2011 Mar;11(2):353–7.
32. Lotinun S, Kiviranta R, Matsubara T, Alzate JA, Neff L, Lüth A, et al. Osteoclast-specific cathepsin K deletion stimulates S1P-dependent bone formation. J Clin Invest. 2013 Feb;123(2):666–81.
33. Winkeler CL, Kladney RD, Maggi LB, Weber JD. Cathepsin K-Cre causes unexpected germline deletion of genes in mice. PLoS ONE. 2012 Jul 31;7(7):e42005.

34. Gowen M, Lazner F, Dodds R, Kapadia R, Feild J, Tavaria M, et al. Cathepsin K knockout mice develop osteopetrosis due to a deficit in matrix degradation but not demineralization. J Bone Miner Res. 1999 Oct;14(10):1654–63.

35. Alfaqeeh S, Oralova V, Foxworthy M, Matalova E, Grigoriadis AE, Tucker AS. Root and Eruption Defects in c-Fos Mice Are Driven by Loss of Osteoclasts. J Dent Res. 2015 Dec;94(12):1724–31.

36. Jiang T, Liu F, Wang W-G, Jiang X, Wen X, Hu K-J, et al. Distribution of cathepsin K in late stage of tooth germ development and its function in degrading enamel matrix proteins in mouse. PLoS ONE. 2017 Jan 17;12(1):e0169857.

37. Kim N, Odgren PR, Kim DK, Marks SC, Choi Y. Diverse roles of the tumor necrosis factor family member TRANCE in skeletal physiology revealed by TRANCE deficiency and partial rescue by a lymphocyte-expressed TRANCE transgene. Proc Natl Acad Sci USA. 2000 Sep 26;97(20):10905–10.

38. Xiong J, Onal M, Jilka RL, Weinstein RS, Manolagas SC, O'Brien CA. Matrix-embedded cells control osteoclast formation. Nat Med. 2011 Sep 11;17(10):1235–41.

39. Sims NA, Martin TJ. Coupling the activities of bone formation and resorption: a multitude of signals within the basic multicellular unit. Bonekey Rep. 2014 Jan 8;3:481.

40. Cheng J, Zhou L, Liu Q, Tickner J, Tan Z, Li X, et al. Cyanidin Chloride inhibits ovariectomy-induced osteoporosis by suppressing RANKL-mediated osteoclastogenesis and associated signaling pathways. J Cell Physiol. 2018 Mar;233(3):2502–12.

41. Park KH, Gu DR, So HS, Kim KJ, Lee SH. Dual Role of Cyanidin-3-glucoside on the Differentiation of Bone Cells. J Dent Res. 2015 Dec;94(12):1676–83.

42. Dou C, Li J, Kang F, Cao Z, Yang X, Jiang H, et al. Dual Effect of Cyanidin on RANKL-Induced Differentiation and Fusion of Osteoclasts. J Cell Physiol. 2016 Mar;231(3):558–67.

43. Moriwaki S, Suzuki K, Muramatsu M, Nomura A, Inoue F, Into T, et al. Delphinidin, one of the major anthocyanidins, prevents bone loss through the inhibition of excessive osteoclastogenesis in osteoporosis model mice. PLoS ONE. 2014 May 13;9(5):e97177.

44. El-Gheriani AA, Maher BS, El-Gheriani AS, et al. Segregation analysis of mandibular prognathism in Libya. *J. Dent. Res.*2003;82(7):523-527. doi:10.1177/154405910308200707.

45. Wiley DF, Amenta N, Alcantara D, et al. Evolutionary Morphing (In Proceedings) . Minneapolis, Minnesota: Proceedings of IEEE Visualization 2005; 2005.

46. Core Team. R: A Language and Environment for Statistical Computing. Vienna, Austria: R Foundation for Statistical Computing; 2012.

47. Kovacs CS. Fetal mineral homeostasis. Pediatric Bone (Second Edition) 2012.

48. Institute of Medicine (US) Standing Committee on the Scientific Evaluation of Dietary Reference Intakes. Dietary Reference Intakes for Calcium, Phosphorus, Magnesium, Vitamin D, and Fluoride. Washington (DC): National Academies Press (US); 1997. doi:10.17226/5776.

49. Donovan PJ, Achong N, Griffin K, Galligan J, Pretorius CJ, McLeod DSA. PTHrP-mediated hypercalcemia: causes and survival in 138 patients. J. Clin. Endocrinol. Metab. 2015;100(5):2024-2029. doi:10.1210/jc.2014-4250.

50. Gallagher JC, Smith LM, Yalamanchili V. Incidence of hypercalciuria and hypercalcemia during vitamin D and calcium supplementation in older women. Menopause 2014;21(11):1173-1180. doi:10.1097/GME.0000000000000270.

51. Hirsch D, Kopel V, Nadler V, Levy S, Toledano Y, Tsvetov G. Pregnancy outcomes in women with primary hyperparathyroidism. J. Clin. Endocrinol. Metab. 2015;100(5):2115 2122. doi:10.1210/jc.2015-1110.

52. Newman EM, Bouvet M, Borgehi S, Herold DA, Deftos LJ. Causes of hypercalcemia in a population of military veterans in the United States. Endocr. Pract. 2006;12(5):535-541. doi:10.4158/EP.12.5.535.

53. Moyers RE, Bookstein FL. The inappropriateness of conventional cephalometrics. Am. J. Orthod. 1979;75(6):599-617.

54. Bookstein FL. Reconsidering “The inappropriateness of conventional cephalometrics”. Am. J. Orthod. Dentofacial Orthop. 2016;149(6):784-797. doi:10.1016/j.ajodo.2015.12.011.

55. Ganpule A, Yajnik CS, Fall CHD, et al. Bone mass in Indian children--relationships to maternal nutritional status and diet during pregnancy: the Pune Maternal Nutrition Study. J. Clin. Endocrinol. Metab. 2006;91(8):2994- 3001. doi:10.1210/jc.2005-2431.

56. Chang S-C, O’Brien KO, Nathanson MS, Caulfield LE, Mancini J, Witter FR. Fetal femur length is influenced by maternal dairy intake in pregnant African American adolescents. Am. J. Clin. Nutr. 2003;77(5):1248-1254. doi:10.1093/ajcn/77.5.1248.

57. Jarjou LMA, Laskey MA, Sawo Y, Goldberg GR, Cole TJ, Prentice A. Effect of calcium supplementation in pregnancy on maternal bone outcomes in women with a low calcium intake. Am. J. Clin. Nutr. 2010;92(2):450-457. doi:10.3945/ajcn.2010.29217.

58. Koo WW, Walters JC, Esterlitz J, Levine RJ, Bush AJ, Sibai B. Maternal calcium supplementation and fetal bone mineralization. Obstet. Gynecol. 1999;94(4):577-582.

59. Kaplan EL, Burrington JD, Klementschitsch P, Taylor J, Deftos L. Primary hyperparathyroidism, pregnancy, and neonatal hypocalcemia. Surgery 1984;96(4):717-722.

60. Robertson WC. Calcium carbonate consumption during pregnancy: an unusual cause of neonatal hypocalcemia. J. Child Neurol. 2002;17(11):853- 855. doi:10.1177/08830738020170111704.

61. Law WM, Heath H. Familial benign hypercalcemia (hypocalciuric hypercalcemia). Clinical and pathogenetic studies in 21 families. Ann. Intern. Med. 1985;102(4):511-519.

62. Kono K, Tanikawa C, Yanagita T, Kamioka H, Yamashiro T. A Novel Method to Detect 3D Mandibular Changes Related to Soft-Diet Feeding. Front. Physiol. 2017;8:567. doi:10.3389/fphys.2017.00567.

63. Anderson PSL, Renaud S, Rayfield EJ. Adaptive plasticity in the mouse mandible. BMC Evol. Biol. 2014;14:85. doi:10.1186/1471-2148-14-85.

Publishing Agreement

It is the policy of the University to encourage the distribution of all theses, dissertations, and manuscripts. Copies of all UCSF theses, dissertations, and manuscripts will be routed to the library via the Graduate Division. The library will make all theses, dissertations, and manuscripts accessible to the public and will preserve these to the best of their abilities, in perpetuity.

Please sign the following statement:

I hereby grant permission to the Graduate Division of the University of California, San Francisco to release copies of my thesis, dissertation, or manuscript to the Campus Library to provide access and preservation, in whole or in part, in perpetuity.

Author Signature

5/28/2019
Date